Nuclear Engineering and Technology 51 (2019) 439–443

Contents lists available at ScienceDirect

Nuclear Engineering and Technology

journal homepage: www.elsevier.com/locate/net

Original Article

Performance evaluation of noise reduction algorithm with median filter using improved thresholding method in pixelated semiconductor gamma camera system: A numerical simulation study

Youngjin Lee

Department of Radiological Science, Gachon University, 191, Hambakmoero, Yeonsu-gu, Incheon, Republic of Korea

ARTICLE INFO

Article history:
Received 5 April 2018
Received in revised form
28 September 2018
Accepted 5 October 2018
Available online 5 October 2018

Keywords:
Medical application
Gamma camera system
Pixelated semiconductor detector
Noise reduction algorithm
Improved median filtering with thresholding method
Monte Carlo simulation

ABSTRACT

To improve the noise characteristics, software-based noise reduction algorithms are widely used in cadmium zinc telluride (CZT) pixelated semiconductor gamma camera system. The purpose of this study was to develop an improved median filtering algorithm using a thresholding method for noise reduction in a CZT pixelated semiconductor gamma camera system. The gamma camera system simulated is a CZT pixelated semiconductor detector with a pixel-matched parallel-hole collimator and the spatial resolution phatnom was designed with the Geant4 Application for Tomography Emission (GATE). In addition, a noise reduction algorithm with a median filter using an improved thresholding method is developed and we applied our proposed algorithm to an acquired spatial resolution phantom image. According to the results, the proposed median filter improved the noise characteristics compared to a conventional median filter. In particular, the average for normalized noise power spectrum, contrast to noise ratio, and coefficient of variation results using the proposed median filter were 10, 1.11, and 1.19 times better than results using conventional median filter, respectively. In conclusion, our results show that the proposed median filter using improved the thresholding method results in high imaging performance when applied in a CZT semiconductor gamma camera system.

1. Introduction

Research in nuclear medicine imaging has actively been studied since *H. Bequerel* discovered natural radioactivity in 1896. The gamma camera system is frequently used in the field of nuclear medicine for cancer detection using the functional imaging technique [1,2]. In this system, patients are injected with radioisotopes (^{99m}Tc is the most commonly used) that emit gamma rays. In general, a NaI(Tl) (3.67 g/cm^3 density) scintillation material, which can be grown with a potassium content of less than 0.5 ppm for low background applications, is one of the most widely used detectors in conventional gamma camera systems because of their lower manufacturing costs and easy crystal growth [3–5].

However, the NaI(Tl) scintillation gamma camera system has the major limitation of relatively poor imaging quality, including low spatial resolution, detection efficiency, and low energy resolution [6]. In addition, based on hygroscopic performance, this system is difficult to manage in room temperature conditions [7]. To address these limitations, a pixelated semiconductor material using cadmium zinc telluride (CZT) or cadmium telluride (CdTe) has been introduced and developed for use in newly-designed detectors [8–11]. The CZT or CdTe pixelated semiconductor detector can acquire images with excellent spatial resolution and has high sensitivity thanks to the small pixel diameters and high density (about 5.80 g/cm^3). According to a previous study, the gamma camera system with a 3-mm thick CZT pixelated semiconductor detector can achieve a resolution of approximately 0.80 mm full width at half maximum (FWHM) and 0.08 counts per second per kBq (cps) using a pixel-matched parallel-hole collimator with 30 mm septal height [12]. When we compared a CZT pixelated semiconductor detector and a NaI(Tl) conventional scintillation detector, the spatial resolution and sensitivity of CZT were 3.81 and 1.52 times higher than those of NaI(Tl), respectively [13]. In addition, a pixelated semiconductor detector can be used at room temperature thanks to its high band-gap energy [14].

However, noise is a major problem in gamma camera imaging systems due to relatively low photon emission [15–17]. This noise in deteriorates the imaging performance and diagnostic accuracy. Thus, noise should be suppressed in order to prevent primary count

E-mail address: yj20@gachon.ac.kr.

https://doi.org/10.1016/j.net.2018.10.005

loss. To cope with this problem, noise reduction algorithms using image processing software have been developed and researched [18–21]. Among these algorithms, application of a median filter to images with noise is one restoration [22]. However, one of the disadvantages of conventional median filtering is the blurring of edge information and loss of image details. Also, although a Wiener filter helped noise stabilization in the frequency domain, this filter also suffers from loss of image details [23]. Therefore, the purpose of this study was to design an improved noise reduction algorithm with a median filter by using a thresholding method in a CZT pixelated semiconductor gamma camera system. For that purpose, we compared our proposed and conventional median filters using the Geant4 Application for Tomographic Emission (GATE) simulation. The normalized noise power spectrum (NNPS), contrast to noise ratio (CNR), and coefficient of variation (COV) were used to evaluate noise reduction ratio.

2. Materials and methods

2.1. Geant4 application for Tomographic Emission (GATE) simulation

Monte Carlo simulations are used extensively to design diagnostic systems and to develop image processing algorithms [24]. Among Monte Carlo simulations, Geant4 is widely used in the field of medical imaging and a tool for modelling the particle passage in the matter. In this study, we used GATE version 7.0 simulation, which is based on the open-source Geant4 software based on the Monte Carlo method [25,26]. For system modelling in the field of nuclear medicine imaging (gamma camera, single photon emission computed tomography (SPECT), and positron emission tomography (PET)), this simulation proved to be very useful in many studies [25–29]. In particular, modelling of radiotherapy, optical imaging, molecular imaging, and nanoparticle-mediated hyperthermal therapy was made possible because of recent GATE simulation advances [30].

2.2. CZT pixelated semiconductor gamma camera system and spatial resolution phantom modelling

We designed a CZT pixelated semiconductor detector (eV-3500, eV product, USA), pixel-matched parallel-hole collimator, and spatial resolution phantom for gamma ray imaging in a GATE simulation (Fig. 2).

The designed CZT pixelated semiconductor detector consisted of linear crystal arrays with 0.5 × 0.5 mm^2 pixel pitch (total detector size: 128 × 0.5 mm^2 (5 × 0.02 $inch^2$)) and 3 mm thickness. The detection efficiency was approximately 72.17 and 58.73% for total and photoelectric absorption at 140 keV gamma ray energy, respectively. Fig. 1 shows the efficiency of the CZT pixelated semiconductor detector with respect to the gamma ray energy.

We simulated a parallel-hole collimator in GATE, which has been widely used for nuclear medicine imaging [31,32]. In our previous study, we showed that high quality images were acquired using a pixel-matched parallel-hole collimator with a pixelated semiconductor detector system among various collimators [33]. Therefore, we designed a pixel-matched parallel-hole collimator for our gamma camera system modelling, which consisted of tungsten because of its lower cost and better image performance [34]. This collimator had a 0.5 mm hole diameter (to equalize detector pixel pitch) and 30 mm septal height.

Finally, we designed a spatial resolution phantom to assess the imaging performance using a solution of ^{99m}Tc gamma source in water with different activities and diameters, and the phantom was acquired with respect to the source-to-collimator distance (1, 3, and 5 cm). This phantom consisted of six different activities and hot-rod diameters: 9000 Bq–0.5 mm, 15,500 Bq–0.85 mm, 30,000 Bq–1.2 mm, 45,000 Bq–1.5 mm, 60,000 Bq–1.8 mm, and 90,000 Bq–2.1 mm.

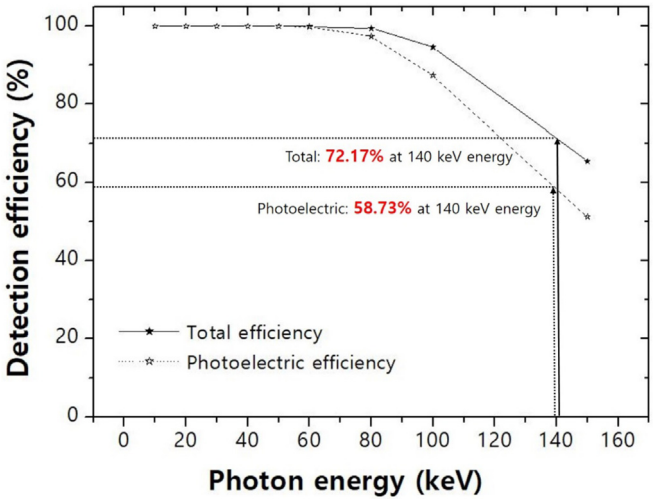

Fig. 1. Graph of the detector efficiency of the CZT pixelated semiconductor material at different gamma ray energies for 3 mm thickness: the total (solid line) and photoelectric (dashed line) efficiencies are shown.

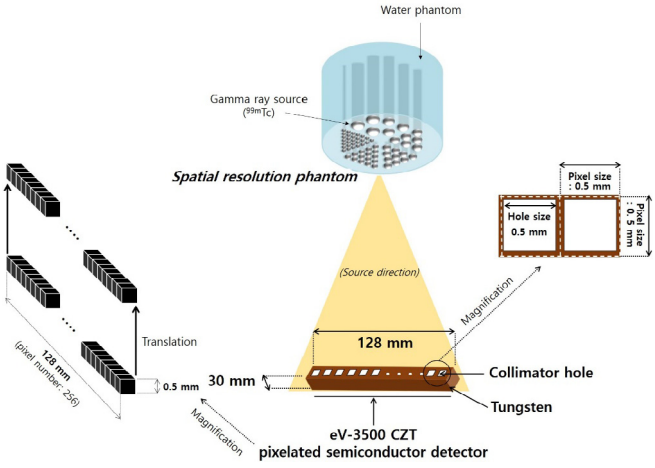

Fig. 2. Schematic description of the simulated pixelated semiconductor gamma camera system with a CZT detector, pixel-matched parallel-hole collimator, and spatial resolution phantom.

2.3. Noise reduction algorithm with median filter using improved thresholding method

We considered a noise reduction algorithm with a median filter using an improved thresholding method to confirm its feasibility for applications in CZT pixelated semiconductor gamma camera systems. The improved thresholding method for noise reduction algorithm modelling can be considered as a special case of de-noising in medical imaging. The concept of this algorithm was proposed by *B. Wang and Q. Pan* [35]. In this study, an improved median filter was suggested to estimate the noise pixels and will be changed by neighboring median pixels. Fig. 3 shows the overall process of the proposed noise reduction algorithm with a median filter using improved the thresholding method. To compare the imaging performance of the de-noising technique, we also

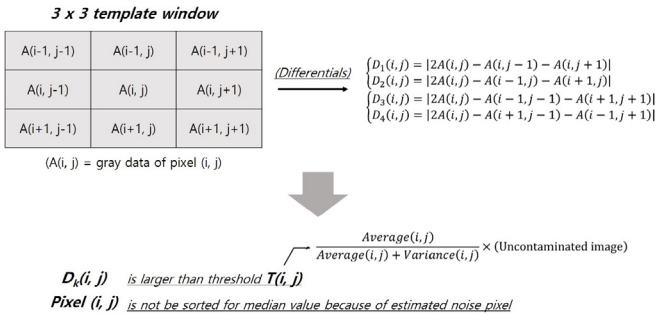

Fig. 3. Schematic flow chart of the designed noise reduction algorithm with median filter and improved thresholding method. This algorithm consists of a thresholding step using the estimated pixel noise.

designed conventional methods using a median filter.

2.4. Quantitative evaluation of image performance

The NNPS, CNR, and COV evaluation parameters were used to evaluate the capability of our designed noise reduction algorithm. To describe the noise characteristics, NNPS ($NPS_{normalized}(u,v)$) is frequently used in medical imaging and is calculated as follows [22]:

$$NPS_{normalized}(u,v) = \frac{NPS(u,v)}{(\text{mean signal of average ROI})^2} \quad (1)$$

$$\left(NPS(u_n,v_k) = \lim_{N_x,N_y\to\infty}(N_xN_y\downarrow x\downarrow y) < |FT_{nk}I(x,y) - S(x,y)|^2 >\right.$$

$$= \lim_{N_xN_y\to\infty}\lim_{M\to\infty}\frac{(N_xN_y\Delta x\Delta y)}{M}\sum_{m=1}^{M}\left|FT_{nk}I(x,y) - S(x,y)\right|^2$$

$$= \lim_{N_xN_y,M\to\infty}\frac{\Delta x\Delta y}{M\cdot N_xN_y}\sum_{m=1}^{M} < \left|\sum_{i=1}^{N_x}\sum_{j=1}^{N_y}\left(I\left(x_i,y_j\right) - S(x,y)\right)\right.$$

$$\left.\left.\exp(-2\pi i(u_nx_i + v_ky_i))\right|^2\right)$$

where u and v are the spatial frequency conjugates in the X and Y directions, respectively; N_x and N_y are the number of pixels in the X and Y directions, respectively; Δx and Δy are the pixel spacing in the X and Y directions, respectively, $I(x_i, y_j)$ is the image intensity at the (x_i, y_j) pixel location, and $S(x, y)$ is the mean intensity.

In addition, the CNR and COV were used to evaluate the contrast, signal, and noise characteristics. The CNR and COV are calculated as follows:

$$CNR = \frac{|S_T - S_B|}{\sqrt{\sigma_T + \sigma_B}} \quad (2)$$

$$COV = \frac{\sigma_T}{S_T} \quad (3)$$

where S_T and σ_T are the mean and standard deviation of the target region of interest (ROI), respectively and S_B and σ_B are mean and the standard deviation for the background ROI, respectively.

3. Results and discussion

The use of gamma rays for nuclear medicine imaging is invaluable and essential for accurate disease detection. Among gamma ray imaging systems, a pixelated semiconductor detector using CZT, which has wide band-gap energy and high density, is very promising. However, the statistical gamma ray interactions between the source and object results in noise when few photons are used to create the image in nuclear medicine imaging systems. Noise reduction is important to achieve improved visualization of small structures and lesions. Many researchers suggested the use of noise reduction algorithms using software techniques to cope with noise problems. Although median filtering was developed first among these algorithms, its noise reduction efficiency ratio is relatively low. Therefore, we designed a noise reduction algorithm with a median filter using an improved thresholding method, which can achieve high noise reduction ratio while retaining more details, and we confirmed the feasibility of this algorithm in a CZT pixelated semiconductor gamma camera system. For that purpose, we simulated an eV-3500 CZT pixelated semiconductor gamma camera system in GATE and evaluated the imaging performance using NNPS, CNR, and COV.

Fig. 4 shows an example of the spatial resolution phantom image with our designed CZT pixelated semiconductor gamma camera system including ROI for measurement of the NNPS (ROI A), CNR (ROI B and ROI C), and COV (ROI B). Fig. 5 shows images with conventional median filtering and our proposed median filter using the improved thresholding method with respect to the source-to-collimator distance.

The calculated NNPS results using conventional median filter and our proposed method at 1 cm source-to-collimator distance are shown in Fig. 6. The NNPS results show that the NNPS value for our proposed median filter method is the lowest (about 10^{-4} mm^2) and approximately 10^2 and 10 times lower than for the noisy image and conventional median filter, respectively. In the NNPS result, we confirmed that our proposed median filter can reduce the noise intensity by to a much greater degree and achieve high imaging

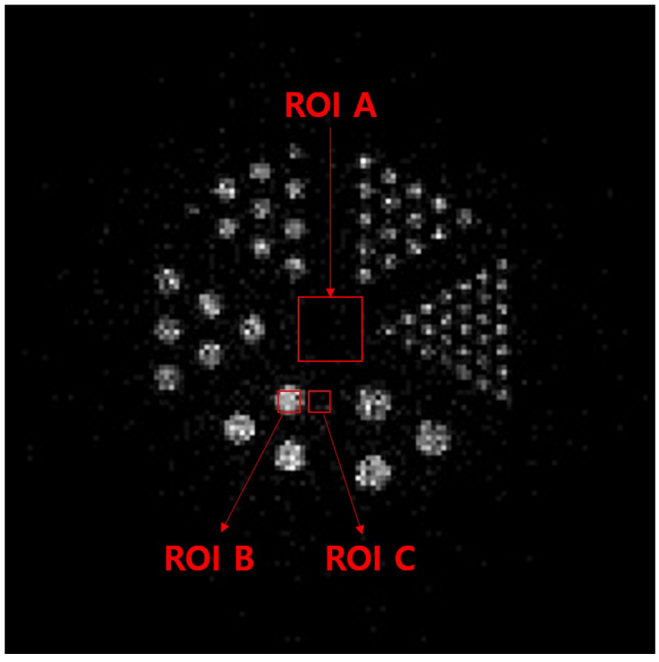

Fig. 4. Example of spatial resolution phantom image with ROIs. The NNPS, CNR, and COV were evaluated after selecting ROI A, ROI B, and ROI C.

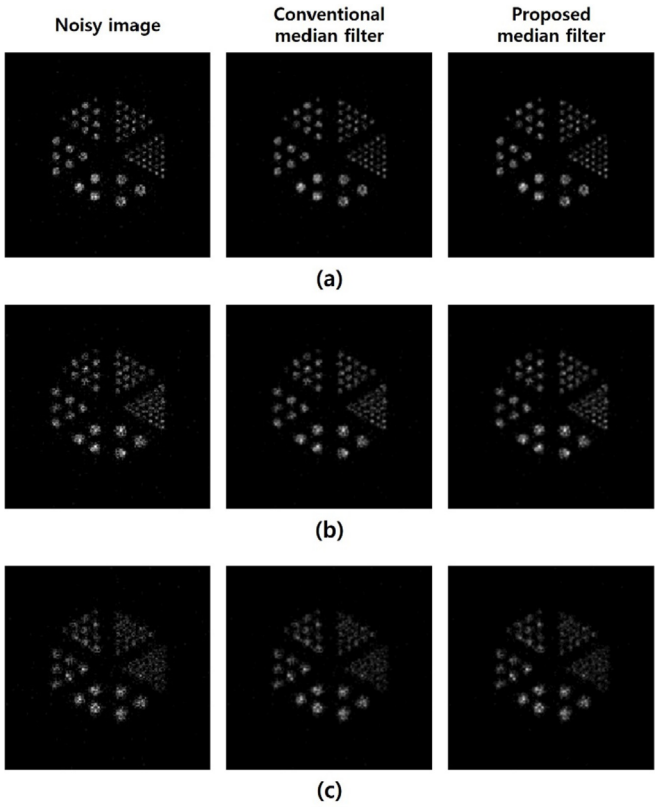

Fig. 5. Simulated images for the noisy, median filter, and proposed median filter with improved thresholding for various source-to-collimator distances: (a) 1 cm, (b) 3 cm, and (c) 5 cm.

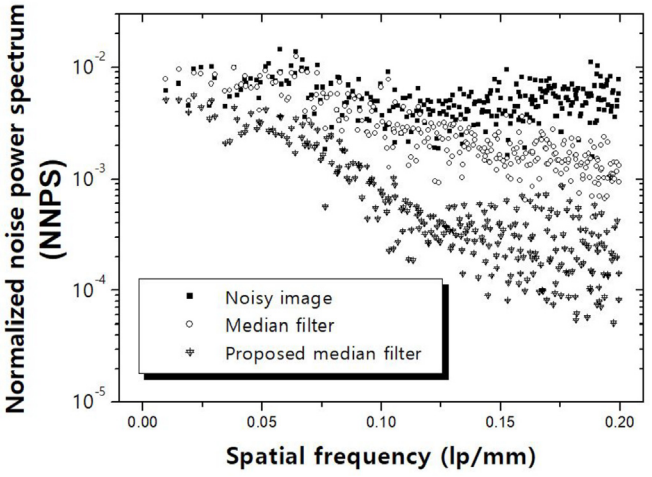

Fig. 6. NNPS results (using ROI A in Fig. 4) for the noisy image, median filter, and proposed median filter with improved thresholding at 1 cm source-to-collimator distance.

performance.

The evaluated CNR results using conventional median filter and our proposed median filtering method as a function of the source-to-collimator distance are shown in Fig. 7. The evaluated CNR obtained from the noisy image, median filter, and our proposed median filter increased in this order. By comparing with noise reduction methods, the CNR result using our proposed median filter was 2.14, 2.26, and 2.59 times higher than that of the noisy

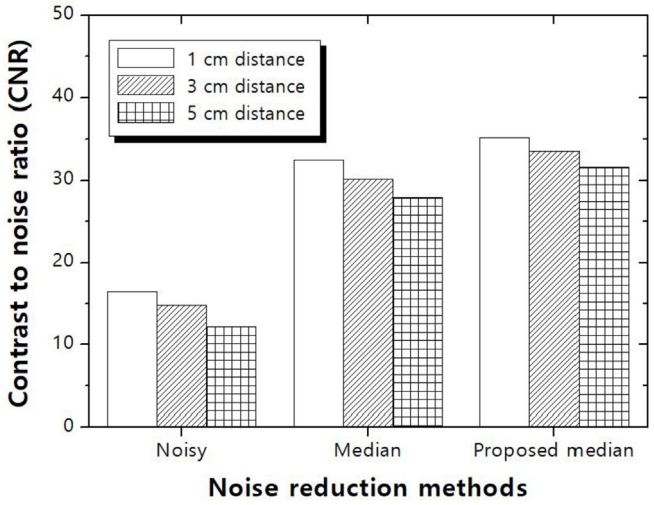

Fig. 7. CNR results (using ROI B and ROI C in Fig. 4) for the noisy image, median filter, and proposed median filter with improved thresholding at 1, 3, and 5 cm source-to-collimator distances.

image at 1, 3, and 5 cm source-to-collimator distances, respectively. In addition, the CNR result using our proposed median filter was 1.08, 1.11, and 1.13 times higher than that of the conventional median filter at 1, 3, and 5 cm source-to-collimator distances, respectively.

The evaluated COV results using the conventional median filter and our proposed median filter method as a function of the source-to-collimator distance are shown in Fig. 8. The evaluated COV obtained from our proposed median filter, the conventional median filter, and the noisy image increased in this order. By comparing the noise reduction methods, the COV result using our proposed median filter was 1.60, 1.64, and 1.66 times higher than that of the noisy image at 1, 3, and 5 cm source-to-collimator distances, respectively. In addition, the COV result using our proposed median filter was 1.13, 1.17, and 1.25 times higher than that of the conventional median filter at 1, 3, and 5 cm source-to-collimator distances, respectively.

According to the results, our proposed median filter using the improved thresholding method is the most suitable and performed exceptionally well in CZT pixelated semiconductor gamma camera systems. Our proposed median filter is applied to the gamma ray images, and the visual appearance after noise reduction improved because of the enhanced threshold approach using differences and

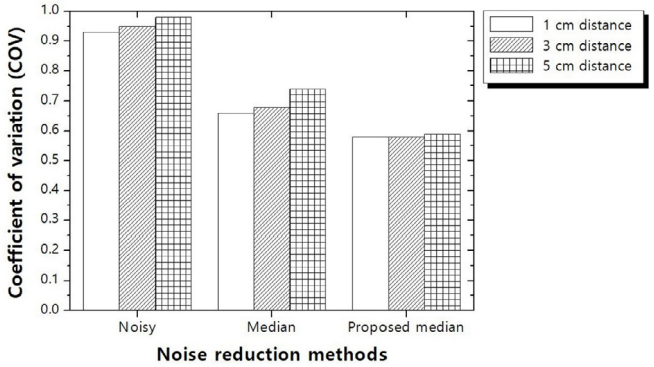

Fig. 8. COV results (using ROI B in Fig. 4) for the noisy image, median filter, and proposed median filter with improved thresholding at 1, 3, and 5 cm source-to-collimator distances.

similar estimated deviation methods. In all cases, the improved imaging performance (NNPS, CNR, and COV) can effectively avoid the influence of mixed noise characteristics. In particular, an analysis of the CNR and COV results showed that our proposed median filter is applied more effectively at a 5 cm than at a 3 cm source-to-collimator distance. This result is due to image performance degradation when we used increasing source-to-collimator distance. In addition, the superior noise characteristics achieved with the proposed median filter in the CZT pixelated semiconductor gamma camera system is expected to provide a lower radiation dose, which is one of the most controversial topics in the field of diagnostic imaging.

4. Conclusion

In this study, the development and implementation of a median filter using an improved thresholding method in a CZT pixelated semiconductor gamma camera system was presented and used to evaluate the noise characteristics using various evaluation parameters. Our results demonstrated that proposed median filter accomplished its goals of noise reduction in CZT gamma camera images.

Acknowledgments

This research was supported by the National Research Foundation of Korea (NRF-2016R1D1A1B03930357).

References

[1] M. Bocher, I.M. Blevis, L. Tsukerman, Y. Shrem, G. Kovalski, L. Volokh, A fast cardiac gamma camera with dynamic SPECT capabilities: design, system validation and future potential, Eur. J. Nucl. Med. Mol. Imag. 37 (2010) 1887–1902.
[2] E.B. Sokole, A. Plachcinska, A. Britten, M.L. Georgosopoulou, W. Tindale, R. Klett, Routine quality control recommendations for nuclear medicine instrumentation, Eur. J. Nucl. Med. Mol. Imag. 37 (2010) 662–671.
[3] H.O. Anger, Scintillation camera with multichannel collimators, J. Nucl. Med. 5 (1964) 515–531.
[4] H. Wieczorek, A. Goedicke, Analytical model for SPECT detector concepts, IEEE Trans. Nucl. Sci. 53 (2006) 1102–1112.
[5] J.H. Kim, Y. Choi, K.S. Joo, B.S. Shin, J.W. Chong, S.E. Kim, K.H. Lee, Y.S. Choe, B.T. Kim, Development of a miniature scintillation camera using an NaI(Tl) scintillator and PSPMT for scintimammograph, Phys. Med. Biol. 45 (2000) 3481–3488.
[6] H.C. Kim, H.J. Kim, K. Kim, M.H. Lee, Y. Lee, Comparison of image uniformity with photon counting and conventional scintillation single-photon emission computed tomography system: a Monte Carlo simulation study, Nucl. Eng. Technol. 49 (2017) 776–780.
[7] P. Yang, C.D. Harmon, F.P. Doty, J.A. Ohlhausen, Effect of humidity on scintillation performance in Na and Tl activated CsI crystals, IEEE Trans. Nucl. Sci. 61 (2014) 1024–1031.
[8] G. Matsumoto, Y. Imura, H. Morii, A. Miyake, T. Aoki, Analysis of artifact with X-ray CT using energy band by photon counting CdTe detector, Nucl. Instrum. Methods Phys. Res. 621 (2010) 292–294.
[9] F. Weng, S. Bagchi, Y. Zan, Q. Huang, Y. Seo, An energy-optimized collimator design for a CZT-based SPECT camera, Nucl. Instrum. Methods Phys. Res. 806 (2016) 330–339.
[10] C. Scheiber, CdTe and CdZnTe detectors in nuclear medicine, Nucl. Instrum. Methods Phys. Res. 448 (2000) 513–524.
[11] K. Ogawa, N. Ohmura, H. Iida, K. Nakamura, T. Nakahara, A. Kubo, Development of an ultra-high resolution SPECT system with a CdTe semiconductor detector, Ann. Nucl. Med. 23 (2009) 763–770.
[12] S. Lee, H.J. Kim, S.Y. Bae, Y. Lee, Experimental study of an easily controlled ultra-high-resolution pixel-matched parallel-hole collimator with a small cadmium zinc telluride pixelated gamma camera system, J. Med. Imag. Radiat. Sci. 47 (2016) 276–282.
[13] Y.J. Lee, S.J. Park, S.W. Lee, D.H. Kim, Y.S. Kim, H.J. Kim, Comparison of photon counting and conventional scintillation detectors in a pinhole SPECT system for small animal imaging: Monte Carlo simulation studies, J. Kor. Phys. Soc. 62 (2013) 1317–1322.
[14] Y.N. Choi, S. Lee, H.J. Kim, Reducing radiation dose by application of optimized low-energy X-ray filters to K-edge imaging with a photon counting detector, Phys. Med. Biol. 61 (2016) N35–N49.
[15] B.S. Bhatia, S.L. Bugby, J.E. Lees, A.C. Perkins, A scheme for assessing the performance characteristics of small field-of-view gamma gameras, Phys. Med. 31 (2015) 98–103.
[16] O. Gal, B. Dessus, F. Jean, F. Laine, C. Leveque, Operation of the CARTOGAM portable gamma camera in a photon-counting mode, IEEE Trans. Nucl. Sci. 48 (2001) 1198–1204.
[17] H. Jeon, H. Kim, C.H. Lee, G. Cho, A simulation study on spatial resolution and noise power spectra of a URA-based multi-hole collimator in a small gamma camera, J. Nucl. Sci. Technol. 5 (2008) 530–533.
[18] P. Chatterjee, P. Milanfar, Is denoising dead? IEEE Trans. Nucl. Sci. 19 (2010) 895–911.
[19] J.T. Dobbins III, E. Samei, N.T. Ranger, Y. Chen, Intercomparison of methods for image quality characterization. II. Noise power spectrum, Med. Phys. 33 (2006) 1466–1475.
[20] X. Zhang, Image denoising using local Wiener filter and its method noise, Optik 127 (2016) 6821–6828.
[21] G. Gao, Y. Liu, An efficient three-stage approach for removing salt & pepper noise from digital images, Optik 126 (2015) 467–471.
[22] K. Seo, S.H. Kim, S.H. Kang, J. Park, C.L. Lee, Y. Lee, The effect of total variation (TV) technique for noise reduction in radio-magnetic X-ray image: quantitative study, J. Magn. 21 (2016) 593–598.
[23] S.H. Kang, K.Y. Kim, Y. Hwang, J.W. Hong, S.R. Baek, C.L. Lee, Y. Lee, A Monte Carlo simulation study for feasibility of total variation (TV) noise reduction technique using digital mouse whole body (MOBY) phantom image, Optik 156 (2018) 197–203.
[24] Y. Lee, A.C. Lee, H.J. Kim, A Monte Carlo simulation study of an improved K-edge log-subtratction X-ray imaging using a photon counting CdTe detector, Nucl. Instrum. Methods Phys. Res. 830 (2016) 381–390.
[25] I. Buvat, I. Castiglioni, Monte Carlo simulations in SPET and PET, Q. J. Nucl. Med. 46 (2002) 48–61.
[26] S. Jan, D. Benoit, E. Becheva, T. Carlier, F. Cassol, P. Descourt, T. Frisson, L. Grevillot, L. Guigues, L. Maigne, C. Morel, Y. Perrot, N. Rehfeld, D. Sarrut, D.R. Schaart, S. Stute, U. Pietrzyk, D. Visvikis, N. Zahra, I. Buvat, GATE V6: a major enhancement of the GATE simulation platform enabling modelling of CT and radiotherapy, Phys. Med. Biol. 56 (2011) 881–901.
[27] C. Robert, N. Fourrier, D. Sarrut, S. Stute, P. Gueth, L. Grevillot, I. Buvat, PET-based dose delivery verification in proton therapy: a GATE based simulation study of five PET system designs in clinical conditions, Phys. Med. Biol. 58 (2013) 6867–6885.
[28] S. Stute, T. Carlier, K. Cristina, C. Noblet, A. Martineau, B. Hutton, L. Barnden, I. Buvat, Monte Carlo simulations of clinical PET and SPECT scans: impact of the input data on the simulated images, Phys. Med. Biol. 56 (2011) 6441–6457.
[29] S. Li, Q. Zhang, Z. Xie, Q. Liu, B. Xu, K. Yang, C. Li, Q. Ren, GATE simulation of a LYSO-based SPECT imager: validation and detector optimization, Nucl. Instrum. Methods Phys. Res. 773 (2015) 21–26.
[30] D. Sarrut, M. Bardies, N. Boussion, N. Freud, S. Jan, J.M. Letang, G. Loudos, L. Maigne, S. Marcatili, T. Mauxion, P. Papadimitroulas, Y. Perrot, U. Pietrzyk, C. Robert, D.R. Schaart, D. Visvikis, I. Buvat, A review of the use and potential of the GATE Monte Carlo simulation code for radiation therapy and dosimetry applications, Med. Phys. 41 (2014), 064301-1-14.
[31] C. Beijst, M. Elschot, M.A. Viergever, H.W.A.M. de jong, A parallel-cone collimator for high-energy SPECT, J. Nucl. Med. 56 (2015) 476–482.
[32] N. Kubo, K. Tsuchiya, T. Shiga, S. Kojima, A. Suzuki, Y. Ueno, K. Kobashi, N. Tamaki, Collimator for variable sensitivity and spatial resolution without the need for exchange, IEEE Trans. Nucl. Sci. 61 (2014) 2489–2493.
[33] Y. Lee, W. Kang, Performance evaluation of high-resolution square parallel-hole collimators with a CZT room temperature pixelated semiconductor SPECT system: a Monte Carlo simulation study, J. Instrum. (2015), https://doi.org/10.1088/1748-0221/10/07/T07004.
[34] Y.J. Lee, H.J. Ryu, S.W. Lee, S.J. Park, H.J. Kim, Comparision of ultra-high-resolution parallel-hole collimator materials based on the CdTe pixelated semiconductor SPECT system, Nucl. Instrum. Methods Phys. Res. 713 (2013) 33–39.
[35] B. Wang, Q. Pan, Soft-threshold histogram weighted filtering with correlativity for high density salt-pepper noise images, Acta Electron. Sin. 35 (2007) 1347–1351.